Experimental Investigation of Scalar Dissipation Rates in Lean Hydrocarbon/Air Premixed Flames

Yung-Cheng Chen and Robert W. Bilger
School of Aerospace, Mechanical and Mechatronic Engineering
University of Sydney
Sydney, NSW 2006 AUSTRALIA
Email: ycchen@mech.eng.usyd.edu.au

ABSTRACT

Instantaneous, three-dimensional scalar dissipation rates of the reaction progress variable are measured in turbulent premixed Bunsen flames of lean hydrocarbon/air mixtures with the two-sheet, two-dimensional Rayleigh scattering technique. The flames investigated are located in the turbulent flame-front regime on a newly proposed combustion diagram for premixed flames. The conditionally-averaged mean scalar dissipation rates, N_ζ, are found to be lower than the calculated laminar values, indicating a locally broadened flame front. In agreement with previous measurements, the maximum of N_ζ decreases strongly with increasing Karlovitz numbers. The conditional probability density functions are close to a log-normal distribution for scalar dissipation rates conditioned at the progress variable value where the scalar dissipation is maximum in unstretched laminar flame calculations. The time scale for the Favre-averaged mean scalar dissipation rate decreases in general across the turbulent flame brush from the unburnt to burnt side.

Keywords : laser rayleigh scattering imaging, scalar dissipation rate, premixed combustion regime diagram.

INTRODUCTION

The scalar dissipation rate of the reaction progress variable, $N \equiv \alpha(\nabla C_T)^2$, is an important but unknown quantity in applying premixed combustion models [1-3] that take into account the effects of turbulence perturbation on local flame-front structures. Here C_T is the progress variable defined from the normalized flame temperature and α is the thermal diffusivity. For mixing-limited premixed combustion of high Reynolds and Damkohler numbers, the mean scalar dissipation rate scales with the mean reaction rate [4]. A thorough validation of the existing proposals [2,5,6] for modeling mean dissipation rates is thus vital to accurate engineering predictions of practical flames. Model assessment and eventual refinement are better performed in premixed flames of simple geometry under controlled

turbulence conditions. Previous measurements in laboratory flames [6,7] have shown that the conditional mean scalar dissipation rate, $N_\zeta \equiv \langle N | C_T = \zeta \rangle$, decreases in general with increasing turbulence levels. This trend is, however, not consistent with analyses [8,9] of some DNS data sets [10-12], in which N_ζ is significantly higher than its laminar values in the preheat zone. This apparent disagreement between current experimental and numerical results indicates that much work is still needed to resolve the issue of flame thinning or thickening at high turbulence levels.

A series of laser-based imaging experiments [13,14] has recently been conducted at the University of Sydney aiming to investigate the effects of turbulence on local, instantaneous premixed flame-front structures. Care has been particularly taken to improve the spatial resolution for measurements of temperature gradients in all three directions with the two-sheet, two-dimensional Rayleigh scattering technique. Experimental data of the three-dimensional scalar dissipation rates are to be reported for lean to stoichiometric hydrocarbon/air [15] and lean hydrogen/air [16] premixed flames in a pilot-stabilized Bunsen burner. In this paper, our specific aim is to provide additional experimental evidence from lean hydrocarbon/air premixed flames. For these lean mixtures, the in-plane spatial resolution is small enough to resolve the local flame-front structure. On the other hand, turbulence levels in these non-reacting flows are high enough such that the flames investigated are far from laminar flamelets. Features of local flame-front distortion and disruption are highlighted in this paper in terms of instantaneous iso-contours of the reaction progress variable. Conditional averages and probability density functions of the scalar dissipation rate are presented. These results are discussed in support of the newly proposed combustion diagram [14] for premixed combustion. In particular, the turbulent flame-front regime, where these flames are located, is emphasized. The time scales for the Favre-averaged mean scalar dissipation rate, $\widetilde{C_T''^2}/\widetilde{N_T}$ are also plotted versus the Favre-averaged mean progress variable, $\widetilde{C_T''^2}$.

EXPERIMENTAL SET-UP

Details about the optical set-up have been described elsewhere [15], and only a brief account is given here. Two laser beams, one at 532 nm and the other at 355 nm, were generated from two separate Nd:YAG lasers for two-sheet Rayleigh scattering (RS) imaging. Before the two laser beams are combined and parallelled with a dichroic mirror, a Galilean-type beam expander is used to slightly converge the 532-nm beam only. This allows the adjustment of both laser beams to be focused at the same point with a single cylindrical lens of 200-mm focal length. Laser sheet thickness at the focal point is checked to be less than 0.1 mm from the marks of laser pulses on a sensitive paper. The center-to-center distance between the two laser sheets is also measured to be $\Delta z = (0.26 \pm 0.02)$ mm within a region 15 mm long.

Two lens-coupled ICCD camera systems are aligned face-to-face to collect the RS signals. Two narrow-band interference filters of 10 nm FWHM and each centered at 355 and 532 nm, are placed in front of the individual camera system. Experimental time resolution is limited by the laser pulse duration of 6 ns. Planar spatial resolution is determined to be (4 ± 1) pixels from the FWHM thickness of a 5 μm diameter wire imaged with the current

camera system. This corresponds to approximately 110 μm at a scaling of $\Delta x = \Delta r = 28$ μm/pix. The matched image is 14.7 mm wide in the radial (r-) direction. The image height in the axial (x-) direction is 5.6 mm for the 355-nm beam and 3.7 mm for the 532-nm beam because of slight beam.

FLAMES AND BURNER

Both the compressed natural gas/air (flame **M3**) and liquefied petroleum-gas/air (flame **P3**) mixtures were investigated at a fixed equivalence ratio of 0.7. The natural gas (CNG) is composed of 88.8% CH_4, 7.8% C_2H_4, 0.2% C_3H_8, 1.9% CO_2, and 1.3% N_2 by volume. The liquefied petroleum-gas (LPG) has more than 88% of C_3H_8 and 10% C_3H_6. A small pilot flame stabilizes the flames investigated on a Bunsen burner. 150 image pairs were collected at a downstream location of 25 mm, where the pilot has negligible effects [13]. The averaged exit velocity is kept constant at 4.9 m/s based on the volumetric flow rate. Turbulence conditions are changed by placing a perforated plug of different hole diameters, d_h, upstream of the burner exit at a distance of d_p. Two plugs (**L**- and **S**-) are used with their dimensions listed in Table 1 below. The blockage ratio, B, and the normalized mean hole spacing, $M/d_h \equiv (\pi d^2/4n)^{1/2}/d_h$, are chosen to be almost the same. Here d = 36 mm is the burner diameter and n is the number of holes in the perforated plug.

Table 1. Plug dimension

	Large (L-)	Small (S-)
d_h (mm)	6	2
n	7	61
B (%)	80.5	81.2
M/d_h	2.0	2.0
d_p (mm)	69	110

The unstretched laminar flame burning velocity, S_L, of the unburnt mixtures is calculated at an ambient temperature of 298 K and 1 atm. The PREMIX code [17] and a C-3 mechanism [18] of 31 species and 82 elementary chemical reactions are used. The laminar thermal flame thickness, $\delta_{th} \equiv (\nabla C_T|_{max})^{-1}$, is taken as the characteristic length scale for the progress variable. The flame residence time, t_F, is thus defined as δ_{th}/S_L. The turbulent time scale, t_t, is l_f/q', where q' is the averaged turbulence intensity, and l_f is the longitudinal integral length scale. These turbulence scales have been measured at x = 25 mm and r = 10 mm in non-reacting air flows [16] and are summarized in Table 2. Based on these characteristic scales, the flames investigated cover a range of Karlovitz numbers, $Ka \equiv (q'/\lambda)t_F$, from 1.91 to 4.09 and Damköhler numbers, $Da \equiv t_t/t_F$, from 1.85 to 3.78. Here $\lambda = l_f\sqrt{15/Re}$ is the Taylor microscale with the Reynolds number $Re = 15Ka^2Da^2$.

DATA REDUCTION

Table 2. Characteristic flame/flow scales

flame	LM3	LP3	SM3	SP3
S_L (m/s)	0.20	0.23	0.20	0.23
δ_{th} (mm)	0.66	0.52	0.66	0.52
t_F (ms)	3.3	2.2	3.3	2.2
N_{max} (1/s)	562	800	562	800
$l_{f,10}$ (1/mm)	8.9	8.9	8.0	8.0
q'_{10} (m/s)	1.46	1.46	1.08	1.08
t_t (ms)	6.1	6.1	7.4	7.4
q'_{10}/S_L	7.30	6.35	5.40	4.70
$l_{f,10}/\delta_{th}$	13.5	17.1	12.1	15.4
l_m (mm)	3.54	2.01	2.38	1.35
Da	1.85	2.70	2.25	3.28
Ka	4.09	2.84	2.75	1.91

Empirical formulas based on laminar flame calculations are used to convert the Rayleigh scattering signals to progress variable values for both the CNG/air [13] and LPG/air [15] premixed flames. These formulas are found to be insensitive to strain rate variations. However, care [13] is needed in processing the conditional-averaged statistics from experimental data to exclude the post-flame regions where ambient air has been mixed with combustion products in turbulent premixed flames.

The three-dimensional scalar dissipation rate at the pixel point (x,r) is defined as

$$N(x, r) = \alpha (x, r) \left| \nabla C_T (x, r) \right|^2$$

where α is obtained from [19]

$$a(x, r) = \frac{2.58 \cdot 10^{-5}}{\rho_u} \left[\frac{T(x, r)}{T_u} \right]^{1.7} \quad [\mathrm{m^2/sec}]$$

with ρ_u and T_u the density and temperature for the unburnt mixture. The three-dimensional progress variable gradient, $|\nabla C_T|$, is calculated on a pixel-by-pixel basis as

$$\sqrt{\left[\frac{C_T(x,r)-C_T(x+\Delta x,r)}{\Delta x}\right]^2+\left[\frac{C_T(x,r)-C_T(x,r+\Delta r)}{\Delta r}\right]^2+\left[\frac{C_T(x,r)-C_{T,2}(x,r)}{\Delta z}\right]^2}$$

Here $C_T(x,r)$ and $C_{T,2}(x,r)$ are progress variable values on each of the two RS laser sheets of the same (x,r) coordinate. To reduce photon noise, smoothing of the progress variable images is applied using a window of 3 by 3 pixels before the calculations of scalar gradients. This window size is smaller than the image spatial resolution of (4 ± 1) pixels, or approximately 110 μm. The Kolmogorov length scales are calculated to be between 55 to 68 μm for the flames investigated. It is thus expected that the current imaging system is able to capture at least 95% of the scalar dissipation.

RESULTS AND DISCUSSION

Figure 1 shows an image pair of instantaneous iso-C_T contours for flame LM3. The iso-contours for C_T values less than 0.5 are clearly not parallel to each other. These contours are stretched into the unburnt mixtures by strong turbulence/flame interactions, causing substantial broadening and disruption of local flame fronts in the preheat zone. An interaction length scale, $l_m = \mathrm{Da}^{-3/2} l_f$, is proposed [14] that characterizes such flame-front broadening. Values of l_m are listed in Table 2 for the flames investigated. For flame LM3, l_m is 3.54 mm, which corresponds well to the distance between the patch of intermediate C_T values of approximately 0.3 and the burnt mixture of $C_T > 0.8$ in Fig 1.

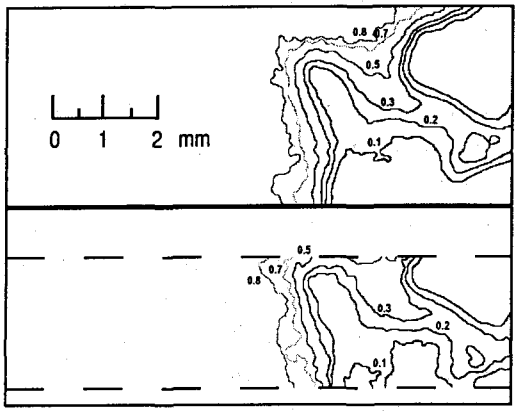

Figure 1. Image pair of instantaneous iso-C_T contours for flame LM3.

The observed flame-front broadening mechanism is dominated via interactions with turbulence of intermediate scales characterized by l_m. This is a distinct feature for premixed flames in the turbulent flame-front regime on a new combustion diagram [14], plotted in

Fig. 2. Locally thickened flame fronts have been reported from recent [14] and previous [6,7] measurements in turbulent premixed flames. These flames are also located in the turbulent flame-front regime, bounded by a lower limit of $l_m > \delta_{th}$ and an upper limit of $l_m < l_f$.

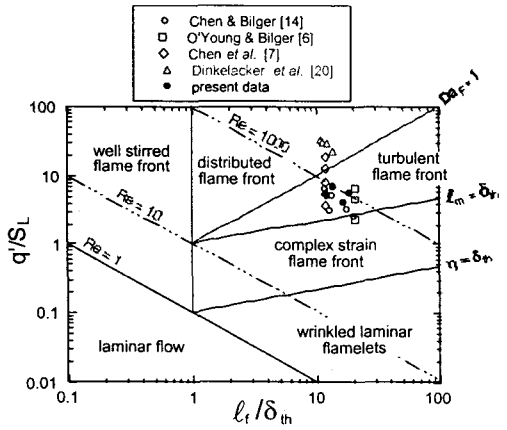

Figure 2. Combustion diagram for turbulent premixed flames.

The local front structures in the turbulent flame-front regime are quite different from laminar flamelet structures because of direct interactions with turbulence. The implications of flame broadening in this regime are important for premixed combustion modelling. Particularly, the scalar dissipation rate for the progress variable, N, declines strongly with increasing turbulence. Figure 3 shows the variation of normalized, conditionally-averaged mean scalar dissipation rates, $N_{\zeta,max}/N_{l,max}$, with Ka. Normalization is made with the maximum scalar dissipation rate from laminar flame calculations, $N_{l,max}$. Values of $N_{l,max}$ are given in Table 2. The present measurements are in good consistency with previous results [15] at the same equivalence ratio of 0.7. However, different dependency on Ka is observed between LPG/air and CNG/air mixtures.

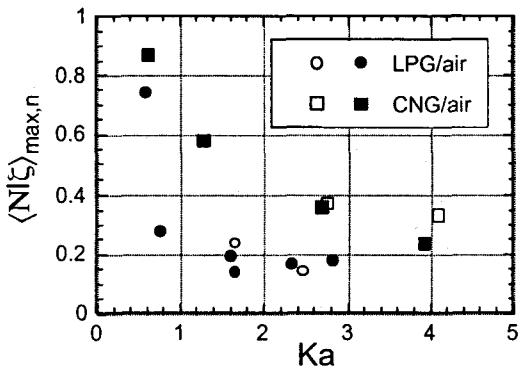

Figure 3. Variation of normalized, conditionally-averaged scalar dissipation rates, $N_{\zeta,max}/N_{l,max}$, with Ka. Open symbols are from the present work and solid symbols are from Ref. [15].

It is noted that Ka equals $C_m(l_m/\delta_{th})$, where C_m is a proportional parameter varied between 0.7 to 0.9 for lean to stoichiometric hydrocarbon/air mixtures. For Ka greater than approximately 1, the interaction length scale l_m is larger than δ_{th}. Turbulence of length scales between l_m and δ_{th} have a time scale smaller than t_F. Thus, local flame front can be perturbed by turbulence within this range before the unburnt mixture can be fully converted into final products. This perturbation creates more intermediate products of progress variable values between 0 and 1 than in laminar flames, and consequently broadens the local flame front as seen in Fig. 1. As a result, the mean scalar dissipation rate decreases strongly when $l_m/\delta_{th} > 1$, or approximately Ka > 1 in Fig. 3.

Figure 4 shows the conditional probability density functions (pdf) for the normalized scalar dissipation rates, N_n, conditioned at the progress variable values where the scalar dissipation is maximum in laminar flame calculations. The normalization is made with $N_{l,max}$. These pdf's appear more like a log-normal

distribution than those from premixed flames of Ka < 1 [15]. A log-normal curve fitting based on the measured mean and rms values shows, however, that the peak position is shifted to larger N_n. A slight skewness towards smaller N_n is also observed at the tails of the pdf distributions.

Figure 5 plots the time scales for the unconditional Favre-averaged scalar dissipation rates, $t_{\widetilde{N}}\,\widetilde{C_T''^2}/\,\widetilde{N}$, versus $\widetilde{C}_T$. A drastic decrease of $t_{\widetilde{N}}$ is observed near the unburnt side of the turbulent flame brush for all the flames investigated. $t_{\widetilde{N}}$ remains almost unchanged within the flame brush and decreases gradually towards the burnt side.

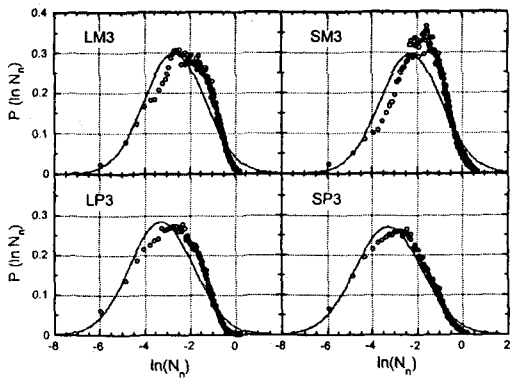

Figure 4. Conditional pdf distributions of the normalized scalar dissipation rates. The solid lines are log-normal curve-fits calculated with the measured mean and rms values.

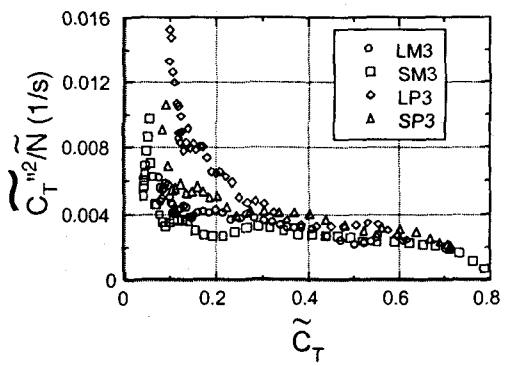

Figure 5. Variation of time scales for the unconditional Favre-averaged scalar dissipation rates, $\widetilde{C_T''^2}/\widetilde{N}$, across the turbulent flame brush.

CONCLUDING REMARKS

Measurements of three-dimensional scalar dissipation rates have been presented for lean hydrocarbon/air premixed Bunsen flames. The Karlovitz number varies between 1.91 and 4.09. For the flames investigated, the iso-C_T contours were substantially disrupted in the preheat zone and the conditionally-averaged mean scalar dissipation rates are smaller than the laminar values. Such flame-front broadening is attributed to direct interactions of the local flame front with turbulence of intermediate length scales between l_m and δ_{th}. The conditional probability density functions of scalar dissipation rates are close to log-normal with small negative skewness. Features of these local flame structures are consistent with premixed flames in the turbulent flame-front regime on the new premixed combustion diagram. A drastic decrease of the time scale, $t_{\widetilde{N}}$, is also found at the leading edge of the turbulent flame brush.

Acknowledgment

This work is supported by the Australian Research Council

REFERENCES

1. Bilger, R. W., in *Turbulence and Molecular Processes in Combustion*, (Takeno, T. Ed.), Elsevier, Amsterdam, 1993, pp. 267-285.
2. Mantel, T. and Borghi, R., *Combust. Flame* 96:443-310 (1994).
3. Vervisch, L., Bidaux, E., Bray, K. N. C., and Kollmann, W., *Phys. Fluids* 7:2496-2503 (1995).

4. Bray, K. N. C., in *Turbulent Reacting Flows* (P. A. Libby and F. A. Williams, Eds.), Springer-Verlag, Heidelberg, 1980, pp. 115-183.
5. Libby, P. A. and Bray, K. N. C., *Combust. Flame* 39:33-41 (1980).
6. O'Young, F. and Bilger, R. W., *Combust. Flame* 109:682-700 (1997).
7. Chen, Y.-C. and Mansour, M. S., *Proc. Combust. Inst.* 27:811-818 (1998).
8. Mantel, T. and Bilger, R. W., *Combust. Sci. and Technol.* 110-111:393-417 (1995).
9. Swaminathan, N., Bilger, R. W., and Cuenot, B., *Combust. Flame* 126:1764-1779 (2001).
10. Trouvé, A. and Poinsot, T. J., *J. Fluid Mech.* 278:1-31 (1994).
11. Baum, M., Poinsot, T. J., Haworth, D. C., and Darabiha, N., *J. Fluid Mech.* 281:1-32 (1994).
12. Echekki, T. and Chen, J. H., *Combust. Flame* 106:184-202 (1996).
13. Chen, Y.-C. and Bilger, R. W., *Combust. Sci. Technol.* 167:131-167 (2001).
14. Chen, Y.-C. and Bilger, R. W., *Combust. Sci. Technol.* 167:187-222 (2001).
15. Chen, Y.-C. and Bilger, R. W., "Experimental Investigation of Instantaneous Flame-Front Structure in Premixed Turbulent Combustion - I: Hydrocarbon/Air Bunsen Flames," submitted to *Combust. Flame* (2002).
16. Chen, Y.-C. and Bilger, R. W., "Experimental Investigation of Instantaneous Flame-Front Structure in Premixed Turbulent Combustion - II: Hydrogen/Air Bunsen Flames," in preparation for *Combust. Flame* (2002).
17. Kee, R. J., Grcar, J. F., Smooke, M.D., and Miller, J. A., "A fortran program for modeling steady laminar one-dimensional premixed flames," *Sandia Report SAND85-8240*, Sandia National Laboratories, Livermore, 1989.
18. Peters, N., in *Reduced Kinetic Mechanisms for Applications in Combustion Systems* (N. Peters and B. Rogg, Eds.), Lecture notes in physics m 15, Springer-Verlag, Heidelberg, 1993, pp. 8-12.
19. Smooke, M. D. and Giovangigli, V., in *Reduced Kinetic Mechanisms and Asymptotic Approximations for Methane-Air Flames*, (M. D. Smooke, Ed.), Springer-Verlag, Heidelberg, 1991, pp. 1-28.
20. Dinkelacker, F., Soika, A., Most, D., Hofmann, D., Leipertz, A., Polifke, W., and Dobbeling, K., *Proc. Combust. Inst.* 27:857-865 (1998).